

PAPER • OPEN ACCESS

Cooling efficiency of gas turbine blade leading edge with a closed whirler

To cite this article: I V Shevchenko *et al* 2018 *J. Phys.: Conf. Ser.* **1128** 012023

View the [article online](#) for updates and enhancements.

You may also like

- [Spatial charge and compensation method in a whirler](#)
Zhenyu WANG, , Binhao JIANG et al.
- [Experimental and Numerical Comparison of Small-scale Gaseous Fire Whirls](#)
Monica Diab, Aaron Yip, Mahshid Hadavand et al.
- [Discussing the rotation movement of an electric whirl through mechanical modelling and video analysis](#)
R S Dutra, J Ataliba, A R Pimenta et al.



ECS
The
Electrochemical
Society
Advancing solid state &
electrochemical science & technology

DISCOVER
how sustainability
intersects with
electrochemistry & solid
state science research

Cooling efficiency of gas turbine blade leading edge with a closed whirler

I V Shevchenko¹, S K Osipov², A N Vegera¹, and I I Komarov²

¹ Department of Innovative Technologies of High-Tech Industries, National Research University “Moscow Power Engineering Institute”, Krasnokazarmennaya 14, Moscow, 111250, Russia

² Innovation Department, National Research University “Moscow Power Engineering Institute”, Krasnokazarmennaya 14, Moscow, 111250, Russia

E-mail: shevchenkoigv@mpei.ru

Abstract. The high temperature gas turbine vane has the leading edge convective cooling. This study discloses investigation of thermal and hydraulic performance of closed whirler, or cyclone edge cooling. Its mass and heat transfer are simulated with the ANSYS CFX model of the leading edge with closed whirler dome. Changes in air supply and discharge orifice areas change the heat transfer distribution. Test results show the influence of the whirler configuration parameters on heat transfer intensity. The obtained criteria equations allow calculations of local and mean heat transfer coefficients with 8% accuracy.

1. Introduction

Whirl or cyclone cooling is an efficient method for cooling gas turbine blade edges. Its concept involves air tangential supply into the blade cooling channel, or the cyclone chamber through orifices or slots. This produces flow swirl which remarkably intensifies heat transfer on the channel internal walls. The cyclone cooling systems attracts the leading gas turbine manufacturers because of the following. Heat transfer in cyclone chambers [1–4] may be much more intensive than in smooth channels, $Nu/Nu_0=4.0$ or even higher which is a very good performance. The traditional intensification methods are related to small vortex generators which remarkably hampers the blade manufacturing.

Now the cyclone blade cooling is well investigated and many of its technical solutions are patented. A cyclone cooling system review may be seen in [5]. The cyclone-stream cooling chamber presented in [6] is of a practical interest. This system involves a system of inclined circular streams that cool the “ram” point of the blade. The inclined streams are formed with a “step” flow separation near inlet and exit orifices. The orifices are displaced along the chamber height which helps the swirl structures generation and boundary layer decay that additionally intensifies the heat exchange. It is worth mentioning that the cyclone systems introduction requires additional investigations [5].

This study is devoted to the closed cyclone analysis and test of thermal and hydraulic performance intended for design of a high temperature turbine vane with the leading edge convective cooling [7–8].

2. Analysis of the cyclone chamber mass and heat transfer

The simulation model of leading edge cyclone chamber (figure 1) involved the ANSYS CFX computer code. The heat transfer analysis approach was conjugated. The first simulated volume is the



metal wall, the second one is the cooling air volume. Two volumes are connected by the heat flux through the metal wall inner surfaces and air volume outer surface. This approach allows the first type boundary conditions on the metal wall outer surface which is in line with the zinc bath test [9].

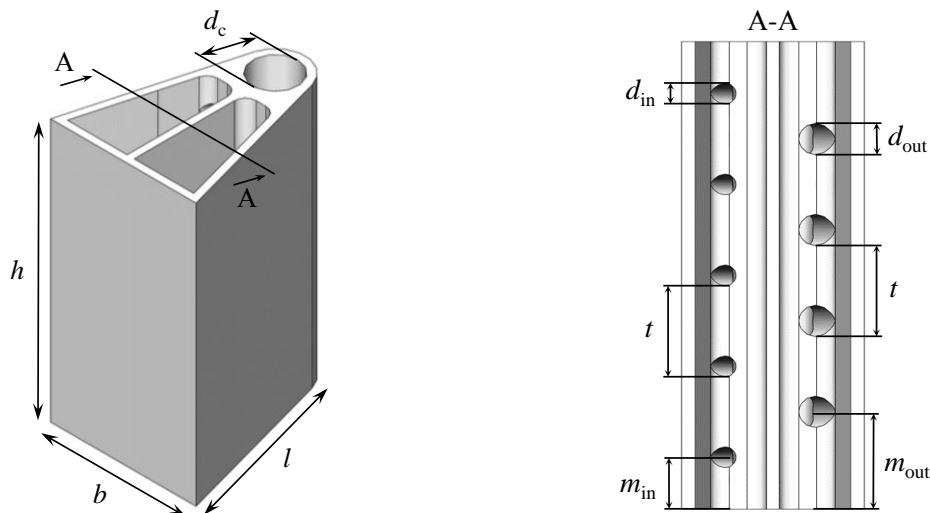


Figure 1. 3D model of cyclone cooled leading edge.

The main model dimensions are summarized in table 1. The ratio of inlet d_{in} and outlet d_{out} orifice diameters was verified within the 2...3 range and cyclone chamber d_c and orifice pitch stayed constant.

The analysis included three values of the model inlet total pressure $P_{in}=1.2; 1.4; 1.6$ bar and constant outlet pressure $P_{out}=1$ bar. The model inlet air temperature was $T_{in}=293$ K, the model outer wall temperature was $T_{out}=692.4$ K.

Table 1. Cooling channel dimensions.

Model	h (mm)	b (mm)	l (mm)	d_c (mm)	d_{in} (mm)	d_{out} (mm)	t (mm)	m_{in} (mm)	m_{out} (mm)
M1	36	20	23	6.2	1.6	2.4	7	4	7.5
M2	36	20	23	6.2	1.2	2.2	7	4	7.5
M3	36	20	23	6.2	2.0	3.0	7	4	7.5
M4	36	20	23	6.2	1.0	3.0	7	4	7.5

Calculations show that the area of supply orifices mostly determines the flow capacity performance. Model M3 has maximal massflow and M4 has minimal supply orifice area and thus minimal massflow throughout the investigated pressure drop P_{in}/P_{out} .

Figure 2 shows the model M1 cyclone chamber streamlines at pressure drop $\pi=P_{in}/P_{out}=1.6$. The maximal flow velocity is seen in supply orifices. Downstream the orifices, the air streams loose stability rapidly at their interaction with the concave channel wall. The stream expansion begins at the chamber inlet, where it loses stability, and the expansion ends near the ram point. This process produces an effective pass over the internal surface.

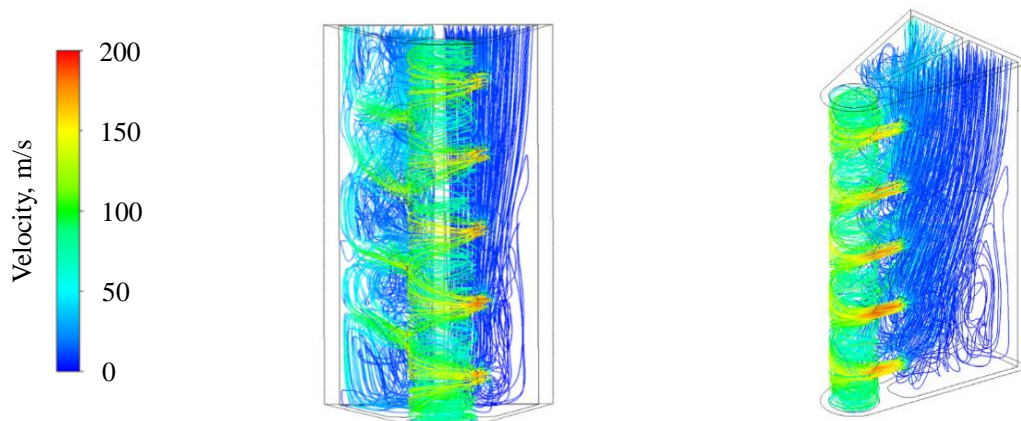


Figure 2. Streamlines in M1 cyclone.

The heat transfer coefficient α was calculated for three points (figure 3). Point 2 is the critical, or ram airfoil point, points 1 and 3 are near the air supply and exit orifices, respectively. Points 1 and 3 are displaced along the channel surface for 45° . Figure 3 shows a distribution example of heat transfer coefficient along the M1 model height at three points for cyclone inlet pressure $P_{in}=1.4$ bar, the horizontal axis reflects the cyclone specific height. The heat transfer has maximal intensity points opposite the supply orifices.

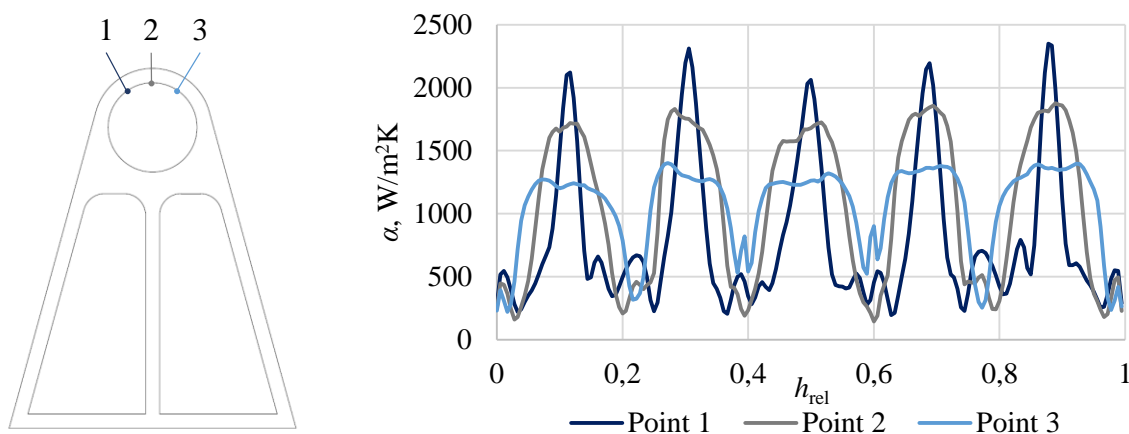


Figure 3. Heat transfer distribution along the M1 model height, $P_{in}=1.4$ bar.

The curve shape reflects the stream extension on the cyclone chamber surface. Near the supply orifices the flow character is nearly streamlike, which produces heat transfer sharp peaks at point 1. Near point 2 the flow spreads over the surface, the peak values drop down, and the curves become smoother.

The computer simulation shows that the ratio of inlet d_{in} and outlet d_{out} increase produces the local heat transfer growth combined with the increase in local heat transfer non-uniformity along the height. Increase in supply and exit orifice areas changes the air flow in cyclone chamber, the stream flow degrades into the flow turn near the cylinder surface.

3. Test of cyclone cooling channel models

3.1. Test models and method

Test models M1, M2 and M3 (table 1) were manufactured by selective laser melting of chromium-nickel alloy with heat conductivity of $16 \text{ W/m}^2\text{K}$. The test method was the liquid metal bath calorimetry [9]. This method is used for investigations of heat transfer performance in convective

cooled blades and cooling channel models. The method physical base is the effect of phase transition in chemically pure metals. The method consists of the following. The cooled blade or the cooling channel model is fitted with air supply and discharge tubes. The model is submerged into the melted zinc bath at the temperatures above the pure zinc crystallization. Then, the model and zinc are cooled down to the equilibrium state at zinc crystallization temperature. The model is blown with the cooling air for time τ and taken out from the melted zinc. On the model surface, there is a metal shell formed by the heat flux to the cooling air in the model channels. Then, the shell thickness is accurately measured at properly located points.

The method accuracy for local heat transfer coefficients is better than $\pm 8\%$. An important feature of this method is the constant thermal load, the model outer surface temperature is equal to zinc crystallization temperature $T_{cr}=692.4$ K [9].

3.2. Models hydraulic performance

The models were cooled with air flow at pressure drops from 1.0 to 4.5 in the melted zinc at the model walls temperature of 692.4 K.

The obtained results show the flow capacity determined by the air supply orifice diameter d_{in} . Model M3 has maximal flow capacity; model M2 has the minimal one. At pressure drop $\pi=3.5$ the model M3 flow is 40% higher than that of the model M2 one.

3.3. Test results analysis, criteria equations

The pressure drop values for the liquid metal bath test were $\pi=1.2$; 1.4; 1.8; 2.2. In terms of the random error reduction each of the tests was five times repeated. Figure 4a (Heat flux distribution along the model M1 cyclone critical line at different cooling air massflows) shows heat flux q distributions along the model M1 height at different cooling air massflow G_{air} values. The plots show that the cooling air massflow increase moves the heat flux q towards its higher values almost equidistantly. The maximal heat flux q points are located against the supply orifices and the minimal flux points are between them. Test results of all models M1, M2 and M3 show the q maximum location near the third orifice along the channel air flow. This effect is caused by the flow velocity and pressure distributions in the channel. The pressure maximum and related orifice velocity maximum correspond to the peripheral section. As the air flow travels along the supply channel, its cooling capacity drops and this causes the smaller heat flux at the last orifices. Thus, the heat flux distribution function $q=f(l)$ is determined by the supply channel pressure distribution, air heating along the channel, orifices number and diameter.

Figure 4b shows the heat flux distribution along the channel perimeter in the $l=21$ mm section at pressure drop 1.8. In this picture the horizontal axis is the angle distance from the zero critical point, the (+) sign shows the air supply orifices perimeter side, the (−) sign shows the exit orifice side.

The heat flux distributions along the model perimeter in models M2 and M3 are nearly equal. The q maximum is located at the critical point and the minimums are at points $+15^\circ$ and -15° . The heat flux at the M2 model similar points is 13–15% higher at all pressure drops. The M1 heat flux distribution is different, at pressure drops of 1.2–1.8 the flux minimum is located at the critical point, at the pressure drop 2.2 the point 0 has a small maximum. As far as the ratio of supply and exit orifices area determines the cyclone chamber flowm it is possible to suppose that smaller F_{in}/F_{out} values move the cyclone flow towards the stream cooling. The smaller exit orifice area forms the flow features like a turn in a curved channel.

At the critical cyclone point, the model M2 has maximal cooling efficiency. At smaller air massflow values the flux q is 15–17% higher than the M1 one. In models M1 and M3 at pressure drops of 1.2 and 1.4, the heat flux values are nearly equal, at pressure drops of 1.8–2.2, the M3 flux is 10–12% smaller.

The criteria equations for heat transfer coefficients use the supply orifice hydraulic diameter d_{in} for the determining dimension. The equations are obtained for the $Re=4000$ –16000 range and the temperature factor of 2.

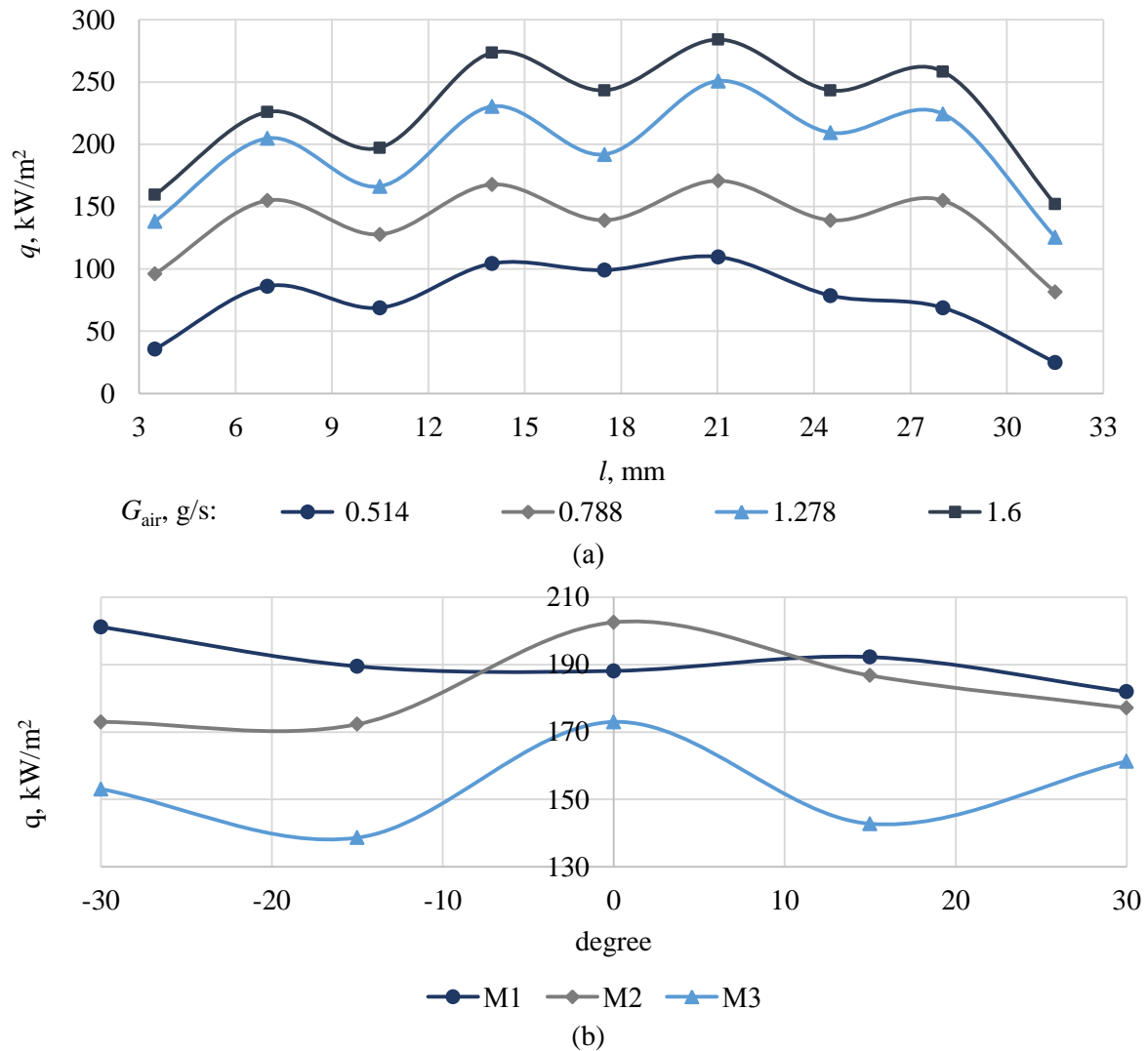


Figure 4. Results of experimental investigation.

The leading edge critical point criteria equation is the following:

$$Nu_0 = 0.21 Re^{0.75} (d_{in} / d_c)^{-0.5} \cdot (F_{in} / F_{out}). \quad (1)$$

The mean heat transfer coefficient of the leading edge perimeter may be calculated through the following equation:

$$Nu_{mean} = 0.20 Re^{0.75} (d_{in} / d_c)^{-0.5} \cdot (F_{in} / F_{out}). \quad (2)$$

The equation above provides the heat exchange calculation error below $\pm 8\%$.

4. Conclusion

1) The computer simulation results show that application of tangential streams produces non-uniform heat transfer along the cyclone chamber height. The heat transfer maximums are located opposite the supply orifices, the minimums are between them. The maximal and minimal heat transfer coefficients

differ more than four times. The non-uniformity may be mitigated by reduction of the supply orifices pitch.

2) The computer simulation results show that an increase in the supply and exit orifices diameters increases local heat transfer coefficients in combination with an increase in heat transfer non-uniformity along the model height. An increase in the supply and exit orifice diameters at constant diameters ratio changes the cyclone chamber internal air flow, the stream flow degrades to a flow turn at the cylinder surface.

3) The liquid metal test results show that two parameters determine the heat transfer distribution along the cyclone chamber surface, the supply and exit orifices diameter ratio, and their total areas ratio. In all tested models, the heat flux reached its maximum around the third orifice along the air supply channel. This heat flux distribution is caused by the pressure distribution along the channel, air heating in the channel, air supply orifices number and diameter. This influence of the supply and exit tubes must be taken into account in the blade cooling analysis.

4) The test results are presented in the form of criteria equations that allow calculation of the leading edge critical point and the mean heat transfer coefficient along the chamber counter with the calculation error below $\pm 8\%$.

Acknowledgments

This study conducted by National Research University “Moscow Power Engineering Institute” has been funded by the Russian Federation through the Ministry of Education and Science of the Russian Federation under Subsidy Agreement No. 14.577.21.0210 of September 28, 2016 as a part of the Federal Targeted Programme for R & D in Priority Fields for the Development of Russia S&T Complex for 2014-2020. Applied Scientific Research Unique Identifier: RFMEFI57716X0210.

References

- [1] Khalatov A., Syred N., Bowen P and Al-Ajmi R 2002 *Proc. Int. Heat Transfer Conf.* (Grenoble, France / Elsevier) pp 662–72
- [2] Ligrani P, Hedlund C, Babinchak B, Thambu R, Moon H and Glezer B 1998 *Exp. Fluids* **24** 254–64
- [3] Thambu R, Babinchak B, Ligrani P, Moon H and Glezer B 1999 *Exp. Fluids* **26** 347–57
- [4] Hedlund C, Ligrani P, Glezer B and Moon H 1999 *Int. J. Heat. Mass. Tran.* **42** 4081–91
- [5] Khalatov A Yu, Dashevsky Ya and Izgoreva I 2008 *Ind. thermal tech.* **30(4)** 14–26
- [6] Fujimoto S, Okita Y and Nakamata C 2009 *Proc. Turbo Expo 2009: Power for Land, Sea, and Air* (Orlando, USA / ASME) pp 723–29
- [7] Shevchenko I V, Rogalev N D, Kindra V O, Osipov S K and Rostova D M 2017 *Int. J. Appl. Eng. Res.* **12(17)** 6853–61
- [8] Shevchenko I V, Rogalev A N, Garanin I V, Vegera A N and Kindra V O 2017 *J. Phys.: Conf. Ser.* **891** 012142
- [9] Shevchenko I V, Rogalev A N, Shevchenko M I and Vegera A N 2017 *Int. J. Appl. Eng. Res.* **12(10)** 2382–86